

# Three-body forces and proton-rich nuclei

J. D. Holt,<sup>1,2</sup> J. Menéndez,<sup>3,4</sup> and A. Schwenk<sup>4,3</sup>

<sup>1</sup>*Department of Physics and Astronomy, University of Tennessee, Knoxville, TN 37996, USA*

<sup>2</sup>*Physics Division, Oak Ridge National Laboratory, P.O. Box 2008, Oak Ridge, TN 37831, USA*

<sup>3</sup>*Institut für Kernphysik, Technische Universität Darmstadt, 64289 Darmstadt, Germany*

<sup>4</sup>*ExtreMe Matter Institute EMMI, GSI Helmholtzzentrum für Schwerionenforschung GmbH, 64291 Darmstadt, Germany*

We present the first study of three-nucleon (3N) forces for proton-rich nuclei along the  $N = 8$  and  $N = 20$  isotones. Our results for the ground-state energies and proton separation energies are in very good agreement with experiment where available, and with the empirical isobaric multiplet mass equation. We predict the spectra for all  $N = 8$  and  $N = 20$  isotones to the proton dripline, which agree well with experiment for  $^{18}\text{Ne}$ ,  $^{19}\text{Na}$ ,  $^{20}\text{Mg}$  and  $^{42}\text{Ti}$ . In all other cases, we provide first predictions based on nuclear forces. Our results are also very promising for studying isospin symmetry breaking in medium-mass nuclei based on chiral effective field theory.

PACS numbers: 21.60.Cs, 21.10.-k, 23.50.+z, 21.30.-x

Exotic nuclei with extreme ratios of neutrons to protons can become increasingly sensitive to new aspects of nuclear forces. This has been shown in shell model studies with three-body forces for the neutron-rich oxygen [1, 2] and calcium [3] isotopes, which present key regions for exploring the evolution to the neutron dripline and for understanding the formation of shell structure. Calculations with three-nucleon forces predicted an increase in binding of the neutron-rich  $^{51,52}\text{Ca}$  isotopes compared to existing experimental values, which was recently confirmed by high-precision Penning-trap mass measurements [4]. The pivotal role of 3N forces has also been highlighted in large-space coupled-cluster calculations [5, 6].

Proton-rich nuclei provide complementary insights to strong interactions, exhibit new forms of radioactivity, and are key for nucleosynthesis processes in astrophysics, such as the rapid-proton-capture process that powers X-ray bursts [7, 8]. Although the proton dripline is significantly better constrained experimentally than the neutron dripline, nuclear forces remain unexplored in medium-mass proton-rich nuclei. Because the proton dripline is closer to the line of stability, it has also been mapped out empirically by calculating the energies of proton-rich systems from known neutron-rich nuclei using the isobaric multiplet mass equation (IMME) [9, 10] or Coulomb displacement energies [11]. This suggests that proton-rich nuclei provide an important testing ground for nuclear forces including known Coulomb and isospin-symmetry-breaking effects.

In this Letter, we present the first study of 3N forces for proton-rich nuclei. The couplings of 3N forces are fit to few-nucleon systems only, and we provide predictions for the ground-state energies (Figs. 1 and 3) and spectra (Figs. 2 and 4) along the chains of  $N = 8$  and  $N = 20$  isotones to the proton dripline. For the interactions studied here, 3N forces provide repulsive contributions as protons are added, similar to the neutron-rich case. This is expected due to the Pauli principle combined with the

leading two-pion-exchange 3N forces [1]. Our results suggest a two-proton-decay candidate  $^{22}\text{Si}$ , whose  $Q$  value is very sensitive to the calculation; within theoretical uncertainties it could also be loosely bound. For the  $N = 20$  isotones, we predict the dripline at  $^{46}\text{Fe}$  and the two-proton emitter  $^{48}\text{Ni}$  [12, 13]. Furthermore, we find good agreement with experimental spectra of  $^{18}\text{Ne}$ ,  $^{19}\text{Na}$ ,  $^{20}\text{Mg}$  and  $^{42}\text{Ti}$  and provide predictions for the isotones where excited states have not been measured.

We consider a shell model description of the  $N = 8$  and  $N = 20$  isotones and determine the interactions among valence protons, on top of a  $^{16}\text{O}$  and  $^{40}\text{Ca}$  core, based on nuclear forces from chiral effective field theory (EFT) [14]. At the NN level, we take the chiral  $\text{N}^3\text{LO}$  potential of Ref. [15] and evolve to a low-momentum interaction  $V_{\text{low } k}$  with cutoff  $\Lambda = 2.0 \text{ fm}^{-1}$  using renormalization-group methods, which improve the many-body convergence [16]. Three-nucleon forces are included at the  $\text{N}^2\text{LO}$  level. These consist of the long-range two-pion-exchange part, as well as one-pion-exchange and short-range contact terms [14]. The shorter-range 3N couplings  $c_D$  and  $c_E$  are determined by fits to the  $^3\text{H}$  binding energy and the  $^4\text{He}$  radius for  $\Lambda_{3\text{N}} = \Lambda = 2.0 \text{ fm}^{-1}$  [17], without further adjustments in the many-body calculations presented here. Note that 3N forces depend on the NN interaction used, so that the contributions from 3N forces differ depending on the cutoff in chiral NN potentials, and when used with bare chiral interactions (see, e.g., Ref. [6]) versus with renormalization-group-evolved interactions.

Excitations outside the valence space are included to third order in many-body perturbation theory (MBPT) [18, 19] in a space of 13 major harmonic-oscillator shells. We have checked that the matrix elements are converged in terms of intermediate-state excitations. For the  $N = 8$  isotones, we consider both the standard  $sd$ -shell and an extended  $sd_{7/2}p_{3/2}$  valence space with  $\hbar\omega = 13.53 \text{ MeV}$ , and for  $N = 20$ , the  $pf$  and  $pf_{g_{3/2}}$  spaces with  $\hbar\omega = 11.48 \text{ MeV}$ . The extended

orbital	emp	MBPT	orbital	emp	MBPT
$d_{5/2}$	-0.60	-0.62/-0.41	$f_{7/2}$	-1.07	-1.16/-0.86
$s_{1/2}$	-0.10	0.82/0.95	$p_{3/2}$	0.63	0.28/1.40
$d_{3/2}$	4.40	4.30/4.57	$p_{1/2}$	2.38	2.40/3.94
$f_{7/2}$		9.73	$f_{5/2}$	5.00	4.91/5.36
$p_{3/2}$		12.64	$g_{9/2}$		6.40

TABLE I. Empirical (emp) and calculated (MBPT in the standard/extended valence spaces) SPEs in MeV.

valence spaces proved important in this framework for oxygen and calcium isotopes [2–4]. In addition to the NN-force contributions, we include the normal-ordered (with respect to the core) one- and two-body parts of 3N forces in 5 major shells [2, 4]. The normal-ordered parts dominate over the contributions from residual three-body interactions [6, 20]. The latter are expected to be weaker in normal Fermi systems due to phase-space limitations in the valence shell compared to the core [21].

For the valence proton single-particle energies (SPEs) in  $^{17}\text{F}$  and  $^{41}\text{Sc}$ , we solve the Dyson equation self-consistently including the contributions from NN and 3N forces in the same spaces and to the same order in MBPT. Our calculated SPEs are given in Table I, in comparison with empirical SPEs taken from the experimental spectra of  $^{17}\text{F}$  and  $^{41}\text{Sc}$ . The MBPT SPEs are similar to the empirical values, but the  $s_{1/2}$  and  $p_{3/2}$  orbitals are at higher energy in both spaces. This finding is similar to the calculated neutron SPEs in oxygen and calcium isotopes [2, 3], which are more bound and differ due to Coulomb and isospin-symmetry-breaking interactions.

All calculations based on NN forces are performed with the empirical SPEs in the standard  $sd$ - and  $pf$ -shells (NN forces only lead to poor SPEs), while those involving 3N forces use MBPT SPEs in both standard and extended valence spaces. In this work, we focus on 3N forces, whose contributions are of the order of a few MeV, but an explicit inclusion of the continuum naturally becomes important for weakly bound states and can lead to very interesting contributions, typically of several hundred keV [5, 22]. Therefore, we only show spectra to  $^{22}\text{Si}$  and to the two-proton emitter  $^{48}\text{Ni}$ . Note that in the case of weakly bound or unbound states, additional attractive contributions from the continuum are expected [22].

We first consider the ground-state energies of the  $N = 8$  isotones from  $^{18}\text{Ne}$  to  $^{24}\text{S}$ , which we compare with experiment when available. As data is limited, we also employ the IMME [9]. This relates the energies in an isospin multiplet (of states with the same quantum numbers in different isobars  $A$ ) by a quadratic dependence in isospin projection  $T_z = (Z - N)/2$ ,

$$E(A, T, T_z) = a(A, T) + b(A, T)T_z + c(A, T)T_z^2. \quad (1)$$

The energies of proton-rich nuclei can thus be obtained from their  $-T_z$  isobaric analogues via  $E(A, T, T_z) =$

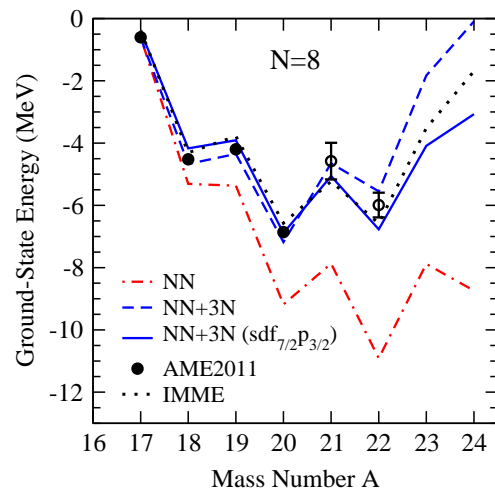


FIG. 1. Ground-state energies of  $N = 8$  isotones relative to  $^{16}\text{O}$ . Experimental energies (AME2011 [23] with extrapolations as open circles) and IMME values are shown. We compare NN-only results in the  $sd$ -shell to calculations based on NN+3N forces in both  $sd$  and  $sd f_{7/2} p_{3/2}$  valence spaces with the consistently calculated SPEs of Table I.

nucleus	$S_p$			$S_{2p}$		
	exp	NN+3N		exp	NN+3N	
$N = 8$	[IMME]	$sd$	$sd f_{7/2} p_{3/2}$	[IMME]	$sd$	$sd f_{7/2} p_{3/2}$
$^{18}\text{Ne}$	3.92	4.05	3.76	4.52	4.67	4.17
$^{19}\text{Na}$	-0.32	-0.32	-0.26	3.60	3.73	3.50
$^{20}\text{Mg}$	2.66	2.83	2.98	2.34	2.51	2.72
$^{21}\text{Al}$	[-1.34]	-2.52	-1.83	[1.45]	0.30	1.15
$^{22}\text{Si}$	[1.35]	0.90	1.71	[0.01]	-1.63	-0.12

TABLE II. Experimental and calculated one- and two-proton separation energies  $S_p$  and  $S_{2p}$  (in MeV) of  $N = 8$  isotones. Where data is unavailable, IMME values are given in brackets.

$E(A, T, -T_z) + 2b(A, T)T_z$ , using a standard fit of the empirical  $b$ -coefficient [9],  $b = (0.7068A^{2/3} - 0.9133)$  MeV, with the atomic mass evaluation (AME2011) [23] for known neutron-rich nuclei. Moreover, we include for comparison the extrapolated values of AME2011, although the IMME is considered to be more accurate.

Figure 1 shows the calculated ground-state energies, obtained from exact diagonalization in the valence spaces with NN-only and NN+3N forces, compared with the AME2011 experimental values and extrapolation, and with the IMME. As expected, the IMME reproduces well experimental data. It finds  $^{22}\text{Si}$  to be bound, though only by 10 keV, with respect to  $^{20}\text{Mg}$ .

In the calculations based on NN forces only, we see a systematic overbinding throughout the isotone chain, which becomes more pronounced for larger mass number. Three-nucleon forces provide key repulsive contributions to ground-state energies and good agreement

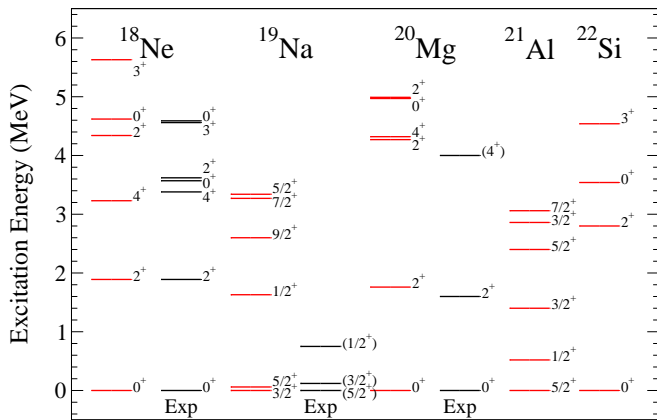


FIG. 2. Excitation energies of  $N = 8$  isotones calculated with NN+3N forces in the  $sdf_{7/2}p_{3/2}$  valence space, compared with experimental data [24–26, 28, 29] where available.

with experiment is obtained in both valence spaces. The extended-space predictions become more bound beyond  $^{20}\text{Mg}$ , the last measured isotone. For both valence spaces, the proton dripline is predicted at  $^{20}\text{Mg}$ , though  $^{22}\text{Si}$  is unbound with respect to  $^{20}\text{Mg}$  by only 0.1 MeV in the extended space, compared with 1.6 MeV in the  $sd$ -shell. This makes a prediction of the dripline difficult, and an experimental measurement of the  $^{22}\text{Si}$  ground-state energy would present a decisive constraint for 3N forces. All calculations find a sharp decrease in binding energy past  $^{22}\text{Si}$ , clearly indicating the dripline has been reached.

A more detailed picture can be developed from the one- and two-proton separation energies given in Table II.  $S_p$  and  $S_{2p}$  are key quantities for determining two-proton emission candidates. In general, we find good agreement between our calculations and the experimental (and IMME) values. While the  $sd$ -shell energies are slightly closer to experiment for lighter isotones, the extended-space calculations agree best with the IMME beyond  $A = 20$ , approximately the same point,  $^{21}\text{O}$ , at which the added valence-space orbitals become important in the oxygen isotopes in this framework [2].

Spectroscopic data in the  $N = 8$  isotones exists to  $^{20}\text{Mg}$ . In Fig. 2, we compare the experimental low-lying states in  $^{18}\text{Ne}$ ,  $^{19}\text{Na}$ , and  $^{20}\text{Mg}$  to those calculated with NN+3N forces in the  $sdf_{7/2}p_{3/2}$  valence space. Calculations with 3N forces in the  $sd$ -shell give very similar spectra up to  $^{19}\text{Na}$ , while for  $^{20}\text{Mg}$ ,  $^{21}\text{Al}$ , and  $^{22}\text{Si}$  they are more compressed than in Fig. 2. In  $^{18}\text{Ne}$  we find good agreement for the first excited  $2^+$  and  $4^+$  states. The ground state and first two excited states in  $^{19}\text{Na}$  have been measured with tentative spin and parity assignments [25, 26]. The ordering of the first two states in our calculation disagrees with the tentative assignments, but the spacing between them is only 0.1 MeV. The  $1/2^+$  state is predicted in our calculation close to the  $1/2^+$  in the mirror  $^{19}\text{O}$ , but 0.9 MeV above experiment. This  $^{19}\text{O}$ - $^{19}\text{Na}$

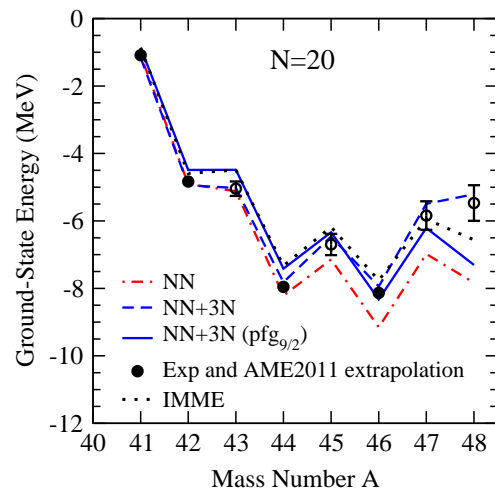


FIG. 3. Ground-state energies of  $N = 20$  isotones relative to  $^{40}\text{Ca}$ . Experimental energies [30] (closed circles) and AME2011 extrapolations [23] (open circles), as well as IMME values are shown. We compare NN-only results in the  $pf$ -shell to calculations based on NN+3N forces in both  $pf$  and  $pfg_{9/2}$  valence spaces with the SPEs of Table I.

nucleus	$S_p$			$S_{2p}$		
	exp	NN+3N		exp	NN+3N	
$N = 20$	[IMME]	$pf$	$pfg_{9/2}$	[IMME]	$pf$	$pfg_{9/2}$
$^{42}\text{Ti}$	3.75	3.78	3.63	4.83	4.94	4.49
$^{43}\text{V}$	[-0.10]	0.09	0.00	[3.62]	3.87	3.62
$^{44}\text{Cr}$	[2.84]	2.79	2.93	3.12	2.88	2.93
$^{45}\text{Mn}$	[-1.15]	-1.35	-1.08	[1.69]	1.44	1.85
$^{46}\text{Fe}$	[1.58]	1.48	1.99	0.18	0.12	0.91
$^{47}\text{Co}$	[-1.81]	-2.45	-2.12	[-0.23]	-0.97	-0.13
$^{48}\text{Ni}$	[0.61]	-0.29	1.09	-1.28(6)	-2.73	-1.02

TABLE III. Experimental and calculated one- and two-proton separation energies  $S_p$  and  $S_{2p}$  (in MeV) of  $N = 20$  isotones. Where data is unavailable, IMME values are given in brackets. Direct measurements of  $S_{2p}$  in  $^{48}\text{Ni}$  are from Refs. [12, 13].

$1/2^+$  difference is a clear example of the Thomas-Ehrman effect [25, 27]. Since in our  $^{19}\text{Na}$  calculation the  $s_{1/2}$  orbital is unbound, continuum coupling is expected to reduce the  $1/2^+$  energy. In  $^{20}\text{Mg}$ , only information on the first excited state has been published [28], but a second excited state has been measured recently [29]. While a tentative assignment of  $4^+$  was given to this state, we predict two close-lying states ( $2^+$  and  $4^+$ ) at very similar energy. In our predictions for  $^{21}\text{Al}$  and  $^{22}\text{Si}$ , we note the high  $2^+$  state in  $^{22}\text{Si}$  as a possible indication of a subshell closure analogous to  $^{22}\text{O}$  [2]. For all cases, the differences of excitation energies between these proton-rich nuclei and the corresponding mirror oxygen isotopes are less than 0.8 MeV.

Next, we show in Fig. 3 the ground-state energies

of the  $N = 20$  isotones from  $^{42}\text{Ti}$  to  $^{48}\text{Ni}$ , where the IMME also reproduces well the limited experimental data [30]. Calculations with NN forces already lead to a reasonable description of experiment, with energies only modestly overbound (within 1 MeV) beyond  $^{45}\text{Mn}$ . When 3N forces are included, the additional repulsion systematically improves the agreement with data. The extended-space calculations agree very well with the IMME throughout the isotone chain, while the  $pf$ -shell results deviate for  $^{47}\text{Co}$  and  $^{48}\text{Ni}$ . In all calculations the proton dripline is robustly predicted at  $^{46}\text{Fe}$ .

The one- and two-proton separation energies are given in Table III. The experimental and IMME values generally fall within the NN+3N calculations in the  $pf$  and  $pf g_{9/2}$  valence spaces. The difference in  $S_p$  and  $S_{2p}$  between the two calculations only becomes larger than 0.7 MeV for  $^{46}\text{Fe}$ ,  $^{47}\text{Co}$  and  $^{48}\text{Ni}$ . This indicates that, in our framework, the  $g_{9/2}$  orbital becomes relevant around  $A = 47$  and provides extra binding, similar to the calcium isotopes [3, 4]. Indeed, our  $pf g_{9/2}$  result for  $S_{2p}$  of  $^{48}\text{Ni}$  is only 0.3 MeV larger than recent experiment [12, 13].

Spectroscopic data is only available for  $^{42}\text{Ti}$  in the  $N = 20$  isotones. We show the predicted spectra based on NN+3N calculations in the  $pf g_{9/2}$  valence space in comparison with experiment in Fig. 4. The energies of the first  $2^+$ ,  $4^+$  and  $6^+$  are well reproduced. There are two observed states between  $2_1^+$  and  $4_1^+$  that do not appear in our calculation. We attribute these to neutron ( $4p2h$ ) excitations, expected around  $^{40}\text{Ca}$  [31]. For the remaining isotones, we show our predictions for the energies of the first five excited states below 5 MeV. Similar to  $^{22}\text{Si}$ , we note the high energy of the  $2^+$  state in  $^{48}\text{Ni}$  as a tentative closed subshell signature. The excitation energy difference with respect to the mirror calcium isotopes is smaller than 0.3 MeV, in agreement with the experimental knowledge in this region [32]. The calculated spectra in the  $pf$ -shell are similar, though modestly compressed, up to  $^{44}\text{Cr}$ , and more compressed beyond.

In summary, we have presented the first study of 3N forces in proton-rich medium-mass nuclei. Our results for ground- and excited-state energies are in very good agreement with experiment, including the prediction of a recently discovered state in  $^{20}\text{Mg}$  [29]. A future measurement of the ground-state energy of  $^{22}\text{Si}$  will provide an important constraint for 3N forces. We make predictions for the unexplored spectra of the  $N = 8$  and  $N = 20$  isotones. Our extended-space calculations for the ground-state energies are of similar quality as empirical IMME predictions, which is very promising for studying isospin symmetry breaking in medium-mass nuclei based on chiral EFT interactions. Our work presents a bridge to future studies, based on nuclear forces, of exotic nuclei with proton and neutron valence degrees of freedom.

We thank M. Pfützner, B. Blank, I. Mukha and A. Poves for helpful discussions, and the TU Darmstadt for hospitality. This work was supported by the US DOE

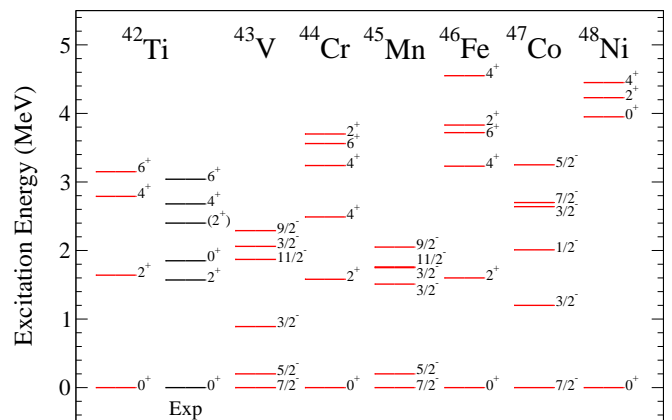


FIG. 4. Excitation energies of  $N = 20$  isotones calculated with NN+3N forces in the  $pf g_{9/2}$  valence space, compared with experiment available for  $^{42}\text{Ti}$  only [24].

Grant DE-FC02-07ER41457 (UNEDF SciDAC Collaboration), DE-FG02-96ER40963 (UT), the Helmholtz Alliance Program of the Helmholtz Association, contract HA216/EMMI “Extremes of Density and Temperature: Cosmic Matter in the Laboratory”, the BMBF under Contract No. 06DA70471, and the DFG Grant SFB 634. Part of the calculations were performed on Kraken at the National Institute for Computational Sciences.

- 
- [1] T. Otsuka *et al.*, Phys. Rev. Lett. **105**, 032501 (2010).
  - [2] J. D. Holt, J. Menéndez and A. Schwenk, arXiv:1108.2680.
  - [3] J. D. Holt *et al.*, J. Phys. G **39**, 085111 (2012).
  - [4] A. T. Gallant *et al.*, Phys. Rev. Lett. **109**, 032506 (2012).
  - [5] G. Hagen *et al.*, Phys. Rev. Lett. **108**, 242501 (2012); *ibid* **109**, 032502 (2012).
  - [6] R. Roth *et al.*, Phys. Rev. Lett. **109**, 052501 (2012).
  - [7] B. Blank and M. J. G. Borge, Prog. Part. Nucl. Phys. **60**, 403 (2008).
  - [8] M. Pfützner *et al.*, Rev. Mod. Phys. **84**, 567 (2012).
  - [9] J. Britz, A. Pape and M. S. Antony, At. Data Nucl. Data Tables **69**, 125 (1998).
  - [10] W. E. Ormand, Phys. Rev. C **55**, 2407 (1997).
  - [11] B. A. Brown *et al.*, Phys. Rev. C **65**, 045802 (2002).
  - [12] C. Dossat *et al.*, Phys. Rev. C **72**, 054315 (2005).
  - [13] M. Pomorski *et al.*, Acta Phys. Pol. B **43**, 267 (2012).
  - [14] E. Epelbaum, H.-W. Hammer and U.-G. Meißner, Rev. Mod. Phys. **81**, 1773 (2009).
  - [15] D. R. Entem and R. Machleidt, Phys. Rev. C **68**, 041001(R) (2003); Phys. Rept. **503**, 1 (2011).
  - [16] S. K. Bogner, T. T. S. Kuo and A. Schwenk, Phys. Rept. **386**, 1 (2003); S. K. Bogner *et al.*, Prog. Part. Nucl. Phys. **65** 94 (2010).
  - [17] K. Hebeler *et al.*, Phys. Rev. C **83** 031301(R) (2010); S. K. Bogner *et al.*, arXiv:0903.3366.
  - [18] B. R. Barrett and M. W. Kirson, in Advances in Nuclear Physics, Vol. 6, p. 219 (Plenum Press, New York, 1973).
  - [19] T. T. S. Kuo and E. Osnes, Springer Lecture Notes of

- Physics, 1990, Vol. 364, p. 1; M. Hjorth-Jensen, T. T. S. Kuo and E. Osnes, Phys. Rept. **261**, 125 (1995).
- [20] G. Hagen *et al.*, Phys. Rev. C **76**, 034302 (2007).
- [21] B. Friman and A. Schwenk, in *From Nuclei to Stars: Festschrift in Honor of Gerald E. Brown*, Ed. S. Lee (World Scientific, 2011) arXiv:1101.4858.
- [22] N. Michel *et al.*, J. Phys. G **37**, 064042 (2010).
- [23] G. Audi and W. Meng, private communication (2011).
- [24] <http://www.nndc.bnl.gov/ensdf/>
- [25] C. Angulo *et al.*, Phys. Rev. C **67**, 014308 (2003).
- [26] I. Mukha *et al.*, Phys. Rev. C **82**, 054315 (2010).
- [27] R. G. Thomas, Phys. Rev. **88**, 1109 (1952); J. B. Ehrman, Phys. Rev. **81**, 412 (1951).
- [28] A. Gade *et al.*, Phys. Rev. C **76**, 024317 (2007).
- [29] I. Mukha, private communication (2012).
- [30] C. Dossat *et al.*, Nucl. Phys. A **792**, 18 (2007).
- [31] W. J. Gerace and A. M. Green, Nucl. Phys. A **93**, 110 (1967).
- [32] M. A. Bentley and S. M. Lenzi, Prog. Part. Nucl. Phys. **59**, 497 (2007).